JOC The Journal of Organic Chemistry

Article

pubs.acs.org/joc

Transition State *Gauche* Effects Control the Torquoselectivities of the Electrocyclizations of Chiral 1-Azatrienes

Ashay Patel,[†] Joseph R. Vella,[†] Zhi-Xiong Ma,[§] R. P. Hsung,*[,§] and K. N. Houk*[,†,‡]

[†]Department of Chemistry and Biochemistry and [‡]Department of Chemical and Biomolecular Engineering, University of California, Los Angeles, California 90095, United States

[§]Division of Pharmaceutical Sciences, School of Pharmacy, and Department of Chemistry, University of Wisconsin, Madison, Wisconsin 53705, United States

Supporting Information

ABSTRACT: Hsung et al. have reported a series of torquoselective electrocyclizations of chiral 1-azahexa-1*E*,3*Z*,5*E*-trienes that yield functionalized dihydropyridines. To understand the origins of the torquoselectivities of these azaelectrocyclizations, we modeled these electrocyclic ring closures using the M06-2X density functional. A new stereochemical model that rationalizes the observed 1,2 stereoinduction emerges from these computations. This model is an improvement and generalization of the "*inside*-alkoxy" model used to rationalize stereoselectivities of the 1,3-dipolar cycloaddition of chiral allyl ethers and emphasizes a stabilizing hyperconjugative effect, which we have termed a transition state *gauche* effect. This stereoelectronic effect controls the conformational preferences at the electrocyclization transition states, and only in one of the allowed disrotatory electrocyclization transition states is the ideal stereoelectronic arrangement achieved without the introduction of a steric clash. Computational experiments confirm the role of this effect as a stereodeterminant since substrates with electropositive groups and electronegative groups have different conformational preferences at the transition state and undergo ring closure with divergent stereochemical outcomes. This predicted reversal of stereoselectivity for the ring closures of several silyl substituted azatrienes have been demonstrated experimentally.

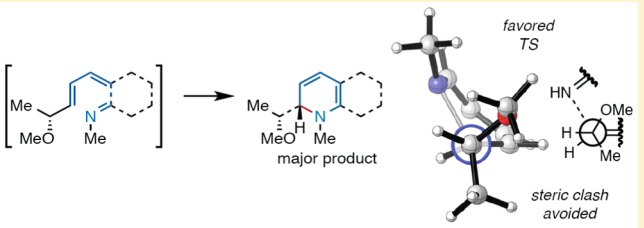

INTRODUCTION

Hsung et al. have demonstrated that an allylic stereocenter can influence the stereochemical outcomes of the disrotatory 6π electrocyclizations of substituted 1-aza-1,3*Z*,5-hexatrienes (summarized in Scheme 1).[1] Here, we report, on the basis of M06-2X/6-31+G(d,p) computations, that *gauche* effects present in the electrocyclization transition states determine the preferred mode of disrotatory ring closure for these chiral 1-azatrienes. In short, the forming C−N bond prefers to maintain a *gauche* relationship with the C−O bond at the allylic stereocenter.

Scheme 1. Torquoselective Electrocyclizations of 1-Aza-1,3*Z*,5-hexatrienes

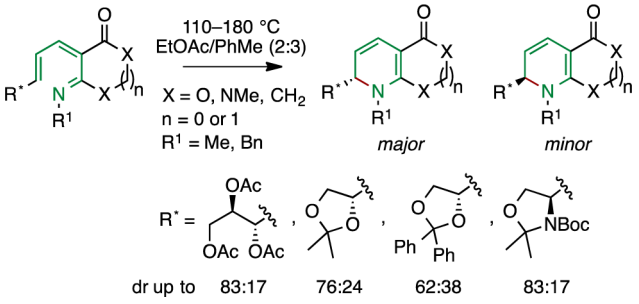

This type of selectivity is a third type of stereoselectivity in the 50 year old history of electrocyclic reactions, celebrated in this issue of the *Journal of Organic Chemistry*. The original formulations of electrocyclic reactions by Woodward and Hoffmann established how the number of electrons involved in bonding changes dictates whether ring closure and opening should be *conrotatory* or *disrotatory*.[2] Our group later developed a theory to understand torquoselectivity, the control of one type of the two possible conrotatory or disrotatory electrocyclizations by terminal substituents.[3−6] The present paper describes how a stereogenic center can influence the torquoselectivity of the electrocyclization.

Ring closures of azatrienes have been examined by a number of researchers,[7−18] and examples of stereoselective azaelectrocyclizations[19−26] have been reported. Despite the utility of the 6π electrocyclization in natural product synthesis and even in biological contexts (i.e., covalent enzyme inhibition and

Special Issue: 50 Years and Counting: The Woodward-Hoffmann Rules in the 21st Century

Received: September 6, 2015
Published: October 4, 2015

ACS Publications © 2015 American Chemical Society

DOI: 10.1021/acs.joc.5b02085
J. Org. Chem. 2015, 80, 11888−11894

biolabeling),[27,28] the origins of the torquoselectivities of these electrocyclizations have yet to be understood. Previous experimental work suggests that electrocyclizations of 1-azatrienes are often reversible at elevated temperatures,[8] unlike the 6π electrocyclization of 1,3*Z*,5-hexatriene. However, experiments suggest that azatrienes shown in Scheme 1 undergo irreversible ring closure;[1] hence, the stereoselectivities of these reactions are under kinetic control.

RESULTS AND DISCUSSION

Figure 1 illustrates the allowed disrotatory transition structures of the ring closures of 1,3,5-hexatriene **1** and those of its 1-aza

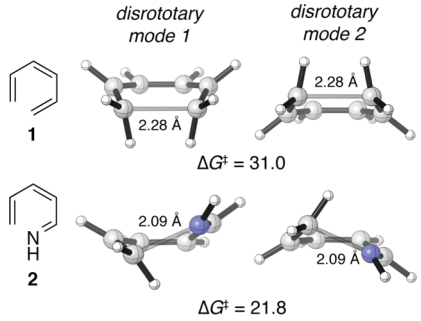

Figure 1. Thermally allowed disrotatory transition structures and activation free energies of the ring closures of 1,3,5-hexatriene and 1-azahexa-1,3,5-triene. Energies are Gibbs free energies in kcal mol^{-1}.

analogue **2**. Whereas the electrocyclization of 1,3,5-hexatriene proceeds through a C_s symmetric boat-like geometry, the transition structures for the corresponding azaelectrocyclization are of lower symmetry; the structures are distorted such that the nitrogen of the azatriene appears to "approach" the C-terminus of the azatriene from above or below the plane of the terminal double bond. According to our previous work, this distortion allows the lone pair of the imine nitrogen to overlap with triene π system, stabilizing the transition state. Lone pair conjugation of this sort is largely responsible for a ~10^7-fold (at 298.15 K, see Figure 1 for free energies of activation) increase in reactivity of 1-azahexa-1,3,5-triene relative to that of 1,3,5-hexatriene.[29]

1-Azatriene **3** is representative of the substrates examined by Hsung and co-workers.[1] It features a number of C−C single bonds capable of free rotation; thus, to reduce the number of conformations that need to be sampled computationally, we examined the simplified trienes, **5a**−**c**, **6**, and **7**, shown in Scheme 2. In all cases, three rotameric transition states were found for each of the disrotatory modes of ring closure (see Figure 2). We labeled these transition states based on the position of the alkoxy substituent with respect the terminal alkene of the azatriene, nomenclature previously used to describe stereoselective additions to alkenes bearing allylic stereocenters.[30]

For both disrotatory modes of ring closure of **5a**, the transition states in which the alkoxy substituent is in the *inside* position (see Figure 2) are most stable. A *gauche* effect is responsible for this conformational preference. In the **TS5a**$_{in1}$ and **TS5a**$_{in2}$, the forming C−N bond and the C−O bond between the alkoxy substituent and the allylic stereocenter are antiperiplanar to σ-donating bonds (C−C and C−H bonds, respectively) and *gauche* to one another. The *anti* transition state conformers **TS5a**$_{anti1}$ and **TS5a**$_{anti2}$, which do not have

Scheme 2. Representative Azaelectrocyclization and Model Substrates Examined Computationally

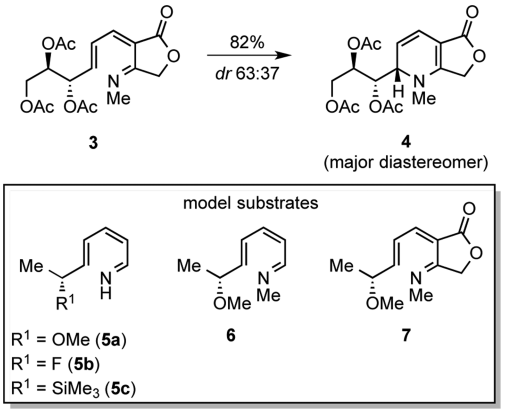

these favorable donor−acceptor interactions, are both about 2 kcal mol^{-1} higher in energy. The *outside*-alkoxy transition states (**TS5a**$_{out1}$ and **TS5a**$_{out2}$) also have a *gauche* arrangement of the C−O and forming C−N bonds and, as a result, are more stable than the *anti* transition structures. However, these transition structures are higher in energy than **TS5a**$_{in1}$ and **TS5a**$_{in2}$ due to electrostatic repulsion between the oxygen of the alkoxy group and the azatriene nitrogen. The O−N interatomic distances in the outside transition state conformer are shorter than those in the corresponding inside transition structures.

The *gauche* effect described above differs from a ground state *gauche* effect[31,32] in that one of the C−X σ acceptors is a bond that is only partially formed in the transition state. For this reason, we have termed this hyperconjugative effect a "transition state *gauche* effect". For these chiral azatrienes, it is the *gauche* relationship between forming C−N and the vicinal C−X bonds at the allylic position of the triene that is ultimately responsible for stereoinduction (Scheme 3). Transition state *gauche* effects of this type are likely general phenomena and may be responsible for the stereoselectivity of other reactions involving alkenes that possess an allylic σ acceptor. The "inside-alkoxy" effect invoked by Houk[30,33−36] and others[37] to rationalize the stereoselectivities of 1,3-dipolar cycloadditions of nitrones and nitrile oxides and chiral allyl ethers is now recognized to be one case of this more general stereochemical model.

To confirm that these stereoelectronic effects are the principal determinants of the transition state conformational preferences of these azaelectrocyclizations, we also modeled the transition states of related substrates **5b** and **5c**, bearing a fluorine or a silyl substituent at the stereogenic center, respectively. If these effects were important, then **5b** (R = F) should have conformational preferences qualitatively similar to those of **5a** at the transition state. Since the $SiMe_3$ group is a hyperconjugative donor,[38] the *anti* transition state conformers of 1-azatriene **5c** should be the most stable: a good donor (C−Si σ bond) is antiperiplanar to the electron-deficient forming C−N bond in the *anti* transition states of **5c**. The $\Delta\Delta G^{\ddagger}$ of all six transition state conformers of **5a**−**c** are summarized in Figure 3.

The conformational preferences of the transition states of **5b** are, indeed, similar to those preferences observed for the transition states of **5a**. The *inside* transition states **TS5b**$_{in1}$ and **TS5b**$_{in2}$ are most stable, and the *anti* transition states are highest in energy. By contrast, we find that the *anti* transition

DOI: 10.1021/acs.joc.5b02085
J. Org. Chem. 2015, 80, 11888−11894

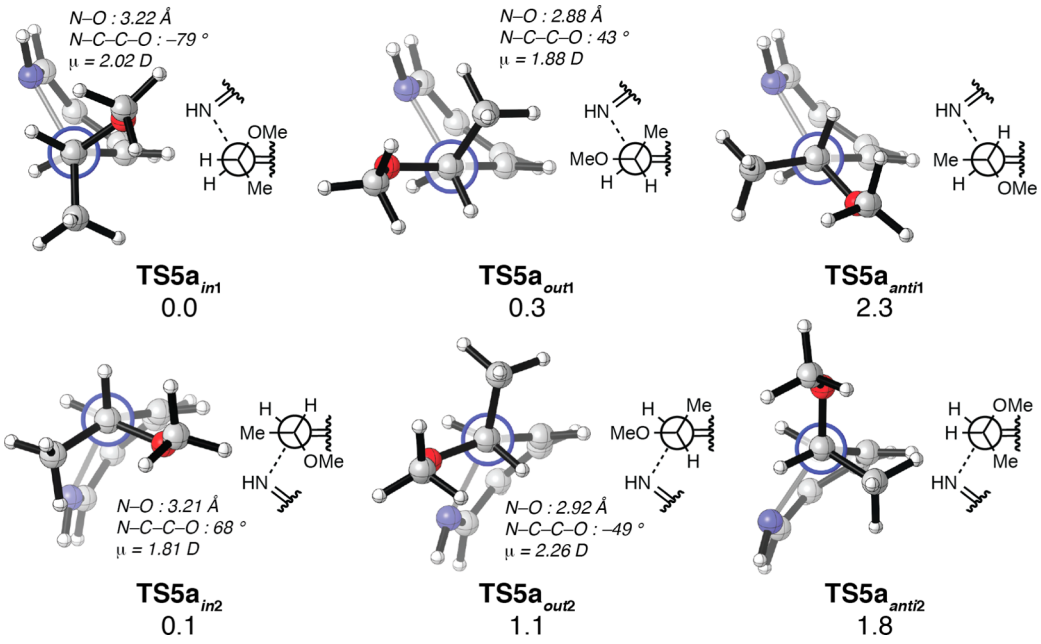

Figure 2. Newman projections of the C5–C6 bond of the M06-2X/6-31+G(d,p)-optimized transition state conformers for the ring closure of **5a**. $\Delta\Delta G^{\ddagger}$ values are reported in kcal mol^{-1}.

Scheme 3. Newman Projections Illustrating the Ground State and Transition State *Gauche* Effects

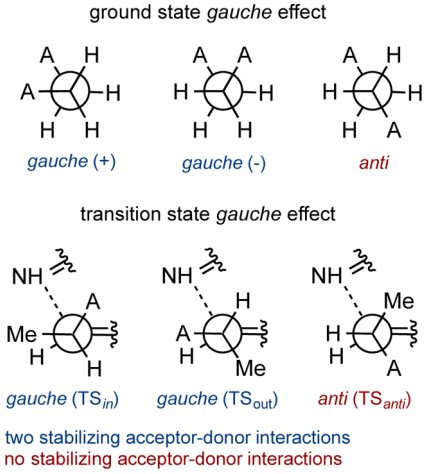

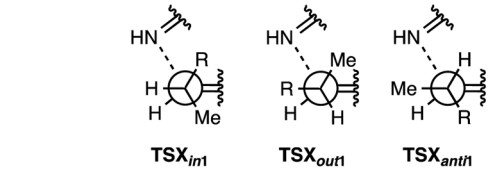

	TSX_{in1}	TSX_{out1}	TSX_{anti1}
5a (R = OMe)	**0.0**	0.3	2.3
5b (R = F)	**0.0**	0.7	2.0
5c (R = SiH_3)	2.5	1.2	**0.5**

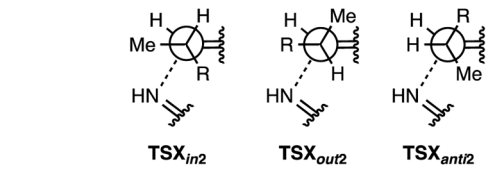

	TSX_{in2}	TSX_{out2}	TSX_{anti2}
5a (R = OMe)	0.1	1.1	1.8
5b (R = F)	0.5	0.8	1.9
5c (R = SiH_3)	1.4	1.8	**0.0**

Figure 3. $\Delta G^{\ddagger}$ differences of the M06-2X/6-31+G(d,p)-optimized ring closure transition state conformers of **5a–c**. $\Delta\Delta G^{\ddagger}$ values were determined relative to inside $\mathbf{TS}_{\mathbf{dis1}}$ for the transition structures of azatrienes **5a** and **5b** and relative to $\mathbf{TS}_{\mathbf{dis2}}$ for the transition structures of **5c**. Energies are reported in kcal mol^{-1}.

state conformers are preferred for the ring closure of **5c** (R = SiH_3), which confirms the nature of the C–N forming bond at the transition state as a hyperconjugative acceptor. This *anti* preference is related to Cieplak's rationalization regarding the origins of π-facial selectivity of nucleophlic additions to cyclic ketones[39,40] and suggests that the nature of bond formation in the electrocyclization, a pericyclic process, is fundamentally different from bond formation in a polar reaction (e.g., nucleophilic acyl addition) for which Cieplak's rationale has been criticized.[41,42]

Experimentally, Hsung et al. have demonstrated that the diastereoselectivities of these azaelectrocyclizations are sensitive to the nature of the N-substituent. To probe this effect, we first examined the transition state conformers of azatriene **6**, bearing a *N*-methyl substituent and then cyclic azatriene **7**. The conformational preferences of **6** remain the same as those found for substrates **5a** and **5b**. According to computations, the two diastereomeric *inside* transition states of azatriene **6** differ in free energy by 1.0 kcal mol^{-1} and are shown in Figure 4. This difference in $\Delta G^{\ddagger}$ is consistent with the sense and level of diastereoselectivity observed experimentally and is caused by a steric clash that destabilizes $\mathbf{TS6}_{\mathbf{in2}}$. In $\mathbf{TS6}_{\mathbf{in2}}$, for the methoxy substituent to occupy its preferred *inside* position, the geminal methyl group must adopt the more sterically demanding *outside* position, whereas in $\mathbf{TS6}_{\mathbf{in1}}$, the hydrogen occupies the *outside* position when the alkoxy is in the *inside* arrangement. That this steric clash involves the *N*-methyl group explains the substituent's importance in stereoinduction.

We next modeled the ring closure of a cyclic azatriene, compound **7** (see Figure 5), which more closely resembles the experimental azatriene **4**. The reaction of the cyclic azatriene **7**

DOI: 10.1021/acs.joc.5b02085
J. Org. Chem. 2015, 80, 11888–11894

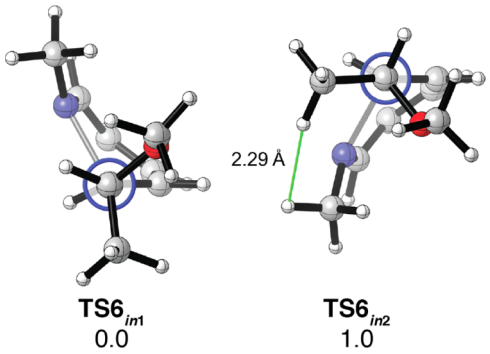

Figure 4. Newman projections of the lowest energy M06-2X/6-31+G(d,p)-optimized 6π electrocyclization transition state conformers of **6**. $\Delta\Delta G^{\ddagger}$ values are given in kcal mol^{-1}.

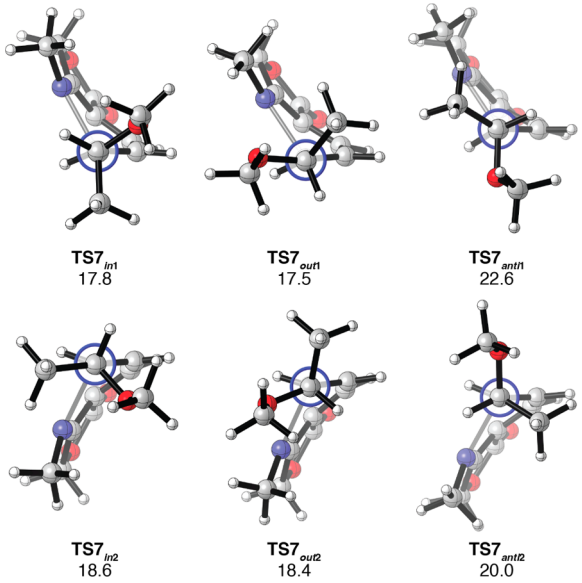

Figure 5. Newman projections of M06-2X/6-31+G(d,p)-optimized transition state conformers of the 6π electrocyclization of azatriene **7**. $\Delta G^{\ddagger}$ are given in kcal mol^{-1}.

proceeds with a barrier of almost 18 kcal mol^{-1} and yields a product that is 16 kcal mol^{-1} more stable than the reactant. Azatriene **7** is more than 10^3-fold more reactive at room temperature ($\Delta\Delta G^{\ddagger}$ = 5 kcal mol^{-1}) than **2a** due to activation by the carbonyl moiety of the lactone and restriction of a rotational degree of freedom by the fused lactone ring. For azatriene **7**, the outside transition states for either mode of ring closure are slightly more stable than the corresponding inside transition states. The subtle change of the conformational preference is due to A^{1,8} strain between the methylene group of the lactone and *N*-methyl of the azatriene in the inside transition state conformers of **7**. Nonetheless, a strong preference for a *gauche* conformation over the *anti* conformation is still predicted. The lowest energy conformers of either mode of disrotation differ by a $\Delta G^{\ddagger}$ of ∼1 kcal mol^{-1}, consistent with the observed diastereoselectivity for the reaction of **3**.

Finally, we return to the silyl derivative **5c**. As discussed above, the silyl group at the allylic position of the azatriene is predicted to reverse the stereoselectivity of the ring closure. This prediction inspired the syntheses and studies of the ring closures of chiral silyl-substituted 1-azatrienes, including **8** (see Scheme 4). The synthesis of silyl-substituted 1-azatrienes and the scope of the ring closures of these compounds are reported

Scheme 4. Electrocyclization of TBPDS-Substituted 1-Azatriene 8[36]

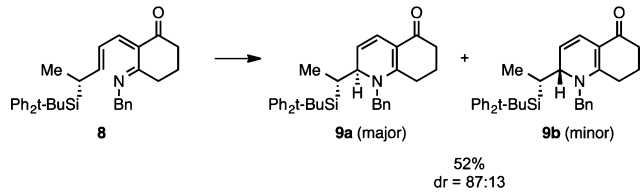

separately.[43] The predicted stereochemical outcome is observed experimentally; however, the ring closure of 1-azatriene **8** is reversible at 130 °C, and over time, the diastereoselectivity of the reaction comes under thermodynamic control. Here we report the origins of the selectivity of the electrocyclization of **8**, using azatriene **10** as a computational model substrate. The results are enumerated in Figure 6.

Just as is the case for the electrocycliczation of **5c**, the *anti* transition state conformers of the ring closure of **10** are lowest in energy. Hyperconjugative stabilization by interaction of the C−Si σ donor orbital with the antibonding σ orbital of the forming C−N bond is likely reinforced by the steric preference of the silyl group for the *anti* position. Computations of the electrocyclic reaction of **10** are consistent with the experimental stereoselectivity; the computed kinetic product **11b** ($\Delta\Delta G^{\ddagger}$ = 2.0 kcal mol^{-1}) corresponds (in terms of relative stereochemistry) to dihydropyridine **9a**.[36] The kinetic diastereoselectivity of the azaelectrocyclization of **10** is also controlled by a steric effect. In **TS10**$_{anti1}$, which leads to the minor product, the methyl substituent at the α position must adopt the *outside* position in order for the TMS group to occupy the *anti* position. In doing so, this methyl group clashes with the N-substituent. This clash is avoided in the favored transition structure **TS10**$_{anti2}$ as the methyl and TMS groups are able to simultaneously occupy the less sterically demanding inside and *anti* positions, respectively.

The equilibration of the two diastereomeric electrocyclization products **11a** and **11b** is observed experimentally, although the major product is still **11b**. The computed $t_{1/2}$ at 130 °C for the ring opening (retroelectrocyclization) of either electrocyclization product is approximately 420 h, too large a value considering that experimental equilibration of the diastereomeric products of electrocyclization occurs within 24 h.[43] The bulky TBDPS group employed experimentally likely accelerates equilibration by destabilizing the products of the electrocyclic ring closure. In any case, the relative energy differences between the two dihydropyridine products indicate that the thermodynamic product is also the kinetic product **11a**.

■ CONCLUSIONS

Transition state *gauche* effects explain the observed stereoselectivities of the electrocyclizations of chiral 1-azatrienes bearing α-alkoxy substituents. Computational experiments predict that an allylic fluorine substituent at the allylic position reproduces the experimentally observed stereoselectivity, while a silyl group at the same position changes the preferred transition state conformation and reverses the stereochemical course of the ring closure. The electrocyclization of TBPDS-substituted azatriene **10** confirms this predicted reversal of selectivity. Studies of the generality of the stereochemical

DOI: 10.1021/acs.joc.5b02085
J. Org. Chem. 2015, 80, 11888−11894

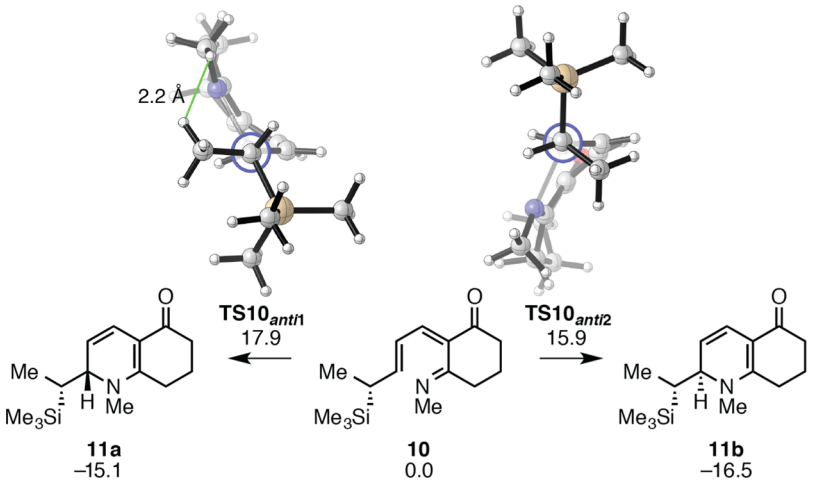

Figure 6. M06-2X/6-31+G(d,p)-optimized transition structures, $\Delta G^{\ddagger}$, and ΔG_{rxn} for the electrocyclization of **10**. Reported energies are in kcal mol^{-1}.

influence of α-silyl groups and the synthetic utility of the ring closures of α-silyl azatrienes have been reported separately.[43]

COMPUTATIONAL METHODS

DFT computations were performed using Gaussian09.[44] The M06-2X[45]/6-31+G(d,p) model chemistry was used to optimize the geometries of stationary points and to compute the vibrational frequencies. M06-2X has been demonstrated to reliably reproduce the thermodynamics of π to σ transformations with reasonable accuracy[46] in addition to the kinetics of main group chemical reactions.[47] All computations were performed in the gas phase. Normal mode analysis confirmed that the optimized structures of reactants and products were minima (zero imaginary frequencies) and that all optimized transition structures corresponded to first-order saddle points (one imaginary frequency). Thermal corrections were calculated from unscaled M06-2X/6-31+G(d,p) frequencies using the standard state conditions of 1 atm and 298.15 K. Errors in the calculation of vibrational entropy contributions to the free energies by the treatment of low modes as harmonic vibrations were mitigated by raising the frequencies of vibrational modes less than 100 cm^{-1} to exactly 100 cm^{-1} as suggested by Truhlar.[48,49] Electronic energies were recomputed at the M06-2X/def2-QZVPP[50,51] level of theory. Reported Gibbs free energies were determined using these electronic energies and thermal corrections determined at the M06-2X/6-31+G(d,p) level. The Avogadro[52,53] and Gaussview[54] software packages were used to build and visualize molecules; the images used in this article were prepared with CYLview.[55] All energies reported are Gibbs free energies in kcal mol^{-1}.

EXPERIMENTAL METHODS

All reactions were performed in flame-dried glassware under a nitrogen atmosphere. Solvents were distilled prior to use. Chromatographic separations were performed using 60 Å SiO_2. ^{1}H and ^{13}C NMR spectra were obtained on spectrometers using $CDCl_3$ with TMS or residual solvent as the standard unless otherwise noted. Infrared spectra were obtained on FTIR, and relative intensities are expressed qualitatively as s (strong), m (medium), and w (weak). TLC analysis was performed using 254 nm polyester-backed plates (60 Å, 250 μm) and visualized using UV and a suitable chemical stain. Low-resolution mass spectra were obtained using LS/MSD APCI, and HRMS was done using ESI. All spectral data obtained for new compounds are reported here.

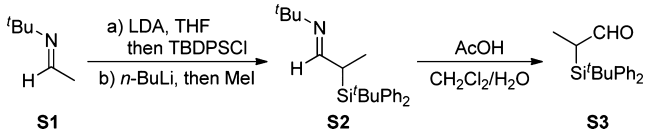

Aldehyde **S3** was prepared (3.50 g, 79%) as a pale yellow liquid following the reported procedure:[56] R_f = 0.55 (hexanes/EtOAc = 5:1); ^{1}H NMR (500 MHz, $CDCl_3$) δ 1.14 (s, 9H), 1.25 (d, J = 7.0 Hz, 3H), 3.09 (dq, J = 2.5, 7.0 Hz, 1H), 7.36–7.44 (m, 6H), 7.58–7.62 (m, 4H), 9.89 (d, J = 2.0 Hz, 1H); ^{13}C NMR (125 MHz, $CDCl_3$) δ 9.7, 19.3, 38.4, 40.3, 127.9 (2 peaks), 129.7 (2 peaks), 132.3, 132.5, 136.0, 136.1, 203.3; IR (thin film) cm^{-1} 3375br, 2093w, 2859w, 1694m, 1427m, 1141w, 1105m; HRMS (QTOF MS ESI) m/e calcd for $C_{19}H_{28}NOSi$ $[M + NH_4]^+$ 314.1935, found 314.1934.

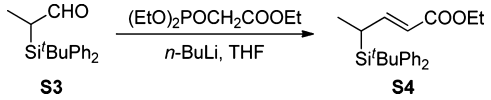

To a solution of $(EtO)_2POCH_2COOEt$ (2.91 g, 13.0 mmol) in THF (20 mL) was added n-BuLi (4.8 mL, 2.5 M in hexanes, 12.0 mmol) at 0 °C. The resulting reaction mixture was kept at this temperature for 30 min before a solution of aldehyde **S3** (2.97 g, 10.0 mmol) in THF (10 mL) was added. The reaction was slowly warmed to rt and then heated at 60 °C overnight. The reaction was quenched with saturated aq NH_4Cl and extracted with EtOAc. The combined organic layers were washed with saturated aq NaCl, dried over Na_2SO_4, filtered, and concentrated under reduced pressure. Purification of the crude residue via silica gel flash column chromatography (isocratic eluent: hexanes/EtOAc = 20:1) gave the pure ester **S4** (3.20 g, 87%) as a pale yellow liquid: R_f = 0.57 (hexanes/EtOAc = 5:1); ^{1}H NMR (400 MHz, $CDCl_3$) δ 1.10 (s, 9H), 1.15 (d, J = 6.8 Hz, 3H), 1.26 (t, J = 7.2 Hz, 3H), 2.65–2.72 (m, ^{1}H), 4.16 (dq, J = 1.2, 7.2 Hz, 2H), 5.61 (dd, J = 1.6, 15.6 Hz, 1H), 7.33–7.45 (m, 7H), 7.57–7.61 (m, 4H); ^{13}C NMR (100 MHz, $CDCl_3$) δ 14.3, 14.4, 19.2, 25.1, 28.5, 59.9, 117.9, 127.6 (2 peaks), 129.3, 129.4, 132.7, 133.3, 136.3, 136.4, 153.5, 166.9; IR (thin film) cm^{-1} 3405br, 2961w, 2858w, 1710s, 1633m, 1470m, 1427w; HRMS (QTOF MS ESI) m/e calcd for $C_{23}H_{34}NO_2Si$ $[M + NH_4]^+$ 384.2354, found 384.2361.

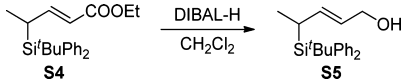

To a solution of ester **S4** (5.20 g, 14.2 mmol) in CH_2Cl_2 (20 mL) was added DIBAL-H (31.3 mL, 1.0 M in hexanes, 31.3 mmol) at −78 °C. The resulting reaction mixture was stirred at this temperature for 30 min, quenched with saturated aq potassium sodium tartrate, and vigorously stirred for another 2 h at room temperature. Then the organic layer was separated, and the aqueous phase was extracted with EtOAc. The combined organic layers were washed with saturated aq NaCl, dried over Na_2SO_4, filtered, and concentrated under reduced pressure. Purification of the crude residue via silica gel flash column

DOI: 10.1021/acs.joc.5b02085
J. Org. Chem. 2015, 80, 11888–11894

chromatography (hexanes/EtOAc = 9:1) gave the pure alcohol **S5** (4.39 g, 95%) as a pale yellow liquid: R_f = 0.40 (hexanes/EtOAc = 3:1); ^{1}H NMR (400 MHz, $CDCl_3$) δ 1.10 (s, 9H), 1.17 (d, J = 7.2 Hz, 3H), 2.45−2.52 (m, 1H), 4.02 (d, J = 6.4 Hz, 2H), 5.43 (dtd, J = 1.6, 6.4, 14.4 Hz, 1H), 5.92 (tdd, J = 1.2, 8.0, 14.4 Hz, 1H), 7.32−7.41 (m, 6H), 7.59−7.60 (m, 2H), 7.61−7.62 (m, 2H); ^{13}C NMR (100 MHz, $CDCl_3$) δ 15.5, 19.1, 23.1, 28.6, 64.2, 126.4, 127.4 (2 peaks), 129.0, 129.1, 133.8, 134.0, 136.4, 13.5, 136.9; IR (thin film) cm^{-1} 3396br, 3957w, 2930w, 2858w, 1655w, 1471w, 1426m, 1265m, 1104s; HRMS (QTOF MS ESI) m/e calcd for $C_{21}H_{32}NOSi$ $[M + NH_4]^+$ 342.2248, found 342.2239.

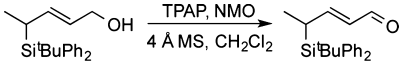

S5 **S6**

To freshly dried 4 Å MS (200 mg) were added a solution of alcohol **S5** (974.0 mg, 3.0 mmol) in CH_2Cl_2 (15 mL), NMO (705.0 mg, 6.0 mmol), and TPAP (52.7 mg, 0.15 mmol) successively in this order. The resulting reaction mixture was stirred for 2 h at ambient temperature, filtered through a small pad of silica gel, and washed with EtOAc. The filtrate was concentrated under reduced pressure. Purification of the crude residue via silica gel flash column chromatography (isocratic eluent: hexanes/EtOAc = 20:1) gave the pure enal **S6** (520.0 mg, 54%) as a pale yellow liquid: R_f = 0.45 (hexanes/EtOAc = 5:1); ^{1}H NMR (500 MHz, $CDCl_3$) δ 1.13 (s, 9H), 1.26 (d, J = 7.0 Hz, 3H), 2.82−2.88 (m, 1H), 5. 93 (ddd, J = 1.5, 8.0, 15.5 Hz, 1H), 7.19 (dd, J = 7.5, 15.5 Hz, 1H), 7.37−7.39 (m, 4H), 7.41−7.45 (m, 2H), 7.56−7.60 (m, 4H), 9.39 (d, J = 7.5 Hz, 1H); ^{13}C NMR (125 MHz, $CDCl_3$) δ 14.4, 19.4, 26.5, 28.6, 127.7, 127.8, 129.6 (2 peaks), 130.1, 132.5 (2 peaks), 136.2 (2 peaks), 164.0, 193.7; IR (thin film) cm^{-1} 3355br, 3072w, 2931w, 2859w, 1681s, 1616m, 1470w, 1427m, 1364w, 1136m, 1104s; HRMS (QTOF MS ESI) m/e calcd for $C_{21}H_{27}OSi$ $[M + H]^+$ 323.1826, found 323.1832.

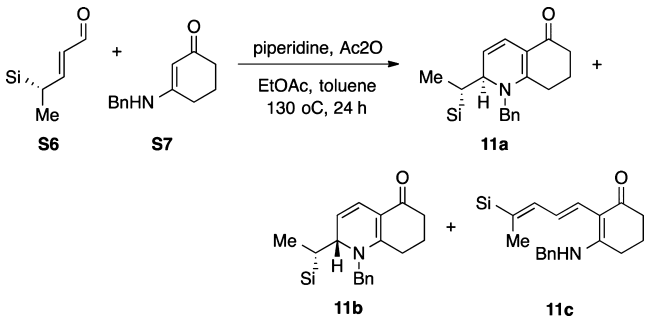

S6 **S7** **11a** **11b** **11c**

The cyclization was performed according to the reported general procedure A[1] at 130 °C for 24 h on a 0.27 mmol scale. The product ratio was determined by ^{1}H NMR analysis of the crude reaction mixture.

11a: 62.0 mg, yield 45%; white solid, mp 62−63 °C; R_f = 0.15 (hexanes/EtOAc = 1:2); ^{1}H NMR (500 MHz, $CDCl_3$) δ 1.01 (s, 9H), 1.31 (d, J = 7.5 Hz, 3H), 1.84−1.92 (m, 2H), 2.01−2.06 (m, 1H), 2.22−2.33 (m, 2H), 2.35−2.41 (m, 1H), 2.45−2.51 (m, 1H), 4.29−4.33 (m, 2H), 4.62 (d, J = 16.5 Hz, 1H), 4.74 (dd, J = 5.0, 10.0 Hz, 1H), 6.62 (d, J = 10.0 Hz, 1H), 7.08−7.10 (m, 2H), 7.24−7.40 (m, 9H), 7.52−7.54 (m, 2H), 7.56−7.58 (m, 2H); ^{13}C NMR (125 MHz, $CDCl_3$) δ 10.1, 18.8, 21.6, 26.5, 26.8, 28.8, 35.5, 52.3, 62.4, 108.3, 112.6, 121.5, 126.1, 127.5, 127.7 (2 peaks), 129.0, 129.2 (2 peaks), 134.1, 134.4, 135.9, 136.6, 136.7, 161.9, 191.4; IR (thin film) cm^{-1} 3398br, 2951w, 2236w, 1737w, 1598m, 1530m, 1472m, 1426m, 1345w; HRMS (QTOF MS ESI) m/e calcd for $C_{34}H_{40}NOSi$ $[M + H]^+$ 506.2874, found 506.2874.

11b: 10.2 mg, yield 7.4%; white solid, mp 57−58 °C; R_f = 0.18 (hexanes/EtOAc = 1:2); ^{1}H NMR (500 MHz, $CDCl_3$) δ 1.04 (s, 9H), 1.33 (d, J = 7.5 Hz, 3H), 1.76−1.83 (m, 2H), 1.85−1.91 (m, 1H), 2.18−2.36 (m, 4H), 3.70 (d, J = 17.0 Hz, 1H), 4.11 (dd, J = 4.5, 5.5 Hz, 1H), 4.22 (d, J = 17.0 Hz, 1H), 5.01 (dd, J = 5.5, 9.5 Hz, 1H), 6.71 (d, J = 9.5 Hz, 1H), 6.73−6.74 (m, 2H), 7.16−7.21 (m, 3H), 7.33−7.46 (m, 6H), 7.64−7.66 (m, 2H), 7.69−7.71 (m, 2H); ^{13}C NMR (125 MHz, CDCl3) δ 11.8, 19.0, 21.4, 26.5, 28.4, 29.0, 35.8, 55.3, 61.6, 111.2, 115.1, 120.4, 125.6, 127.2, 127.6, 127.8, 128.7, 129.3 (2 peaks), 134.2, 134.5, 136.2, 136.4, 137.1, 161.0, 192.0; IR (thin film) cm^{-1} 3398br, 3050w, 2926m, 2856m, 1692w, 1615s, 1536s, 1494w, 1471m, 1426s, 1342m; HRMS (QTOF MS ESI) m/e calcd for $C_{34}H_{40}NOSi$ $[M + H]^+$ 506.2874, found 506.2874.

11c: 6.0 mg, yield 4.3%; white solid, mp 82−83 °C; R_f = 0.40 (hexanes/EtOAc = 1:2); ^{1}H NMR (500 MHz, $CDCl_3$) δ 1.12 (s, 9H), 1.86 (d, J = 1.5 Hz, 3H), 1.90−1.95 (m, 2H), 2.36 (t, J = 6.5 Hz, 2H), 2.56 (t, J = 6.0 Hz, 2H), 4.49 (d, J = 6.0 Hz, 2H), 5.96 (t, J = 5.5 Hz, 1H), 6.42 (d, J = 16.0 Hz, 1H), 6.58 (dd, J = 2.0, 11.0 Hz, 1H), 7.07 (dd, J = 10.5, 16.0 Hz, 1H), 7.26−7.28 (m, 3H), 7.31−7.34 (m, 5H), 7.35−7.40 (m, 4H), 7.53−7.54 (m, 2H), 7.55 (m, 2H); ^{13}C NMR (125 MHz, $CDCl_3$) δ 17.6, 18.7, 20.4, 26.1, 29.0, 36.7, 47.3, 108.7, 126.1, 126.7, 126.8, 127.6, 128.0, 128.9, 129.1, 131.8, 134.9, 136.3, 137.4, 144.2, 162.1, 194.1; IR (thin film) cm^{-1} 3386br, 2930w, 2857w, 1621w, 1550m, 1454w, 1426m, 408m, 1354w; HRMS (QTOF MS ESI) m/e calcd for $C_{34}H_{40}NOSi$ $[M + H]^+$ 506.2874, found 506.2883.

■ ASSOCIATED CONTENT

Supporting Information

The Supporting Information is available free of charge on the ACS Publications website at DOI: 10.1021/acs.joc.5b02085.

Cartesian coordinates, zero-point energy, thermal and quasiharmonic corrections for all computed structures, and imaginary frequencies of the transition states (PDF)
Proton and carbon NMR spectra (PDF)

■ AUTHOR INFORMATION

Corresponding Authors

*E-mail: rphsung@pharmacy.wisc.edu.
*E-mail: houk@chem.ucla.edu.

Notes

The authors declare no competing financial interest.

■ ACKNOWLEDGMENTS

We acknowledge the financial support of the NIH (GM-66055 to R.P.H., GM-36700 and CHE-1351104 to K.N.H.) A.P. thanks the Chemical-Biology Interface Training Program for its support (T32 GM 008496). A.P. and J.R.V. acknowledge the University of California, Los Angeles, and the Amgen Scholars Program, respectively, for financial support. This work used computational and storage services associated with the Hoffman2 Shared Cluster provided by UCLA Institute for Digital Research and Education's Research Technology Group in addition to the NSF-supported Extreme Science and Engineering Discovery Environment (XSEDE)'s Trestles and Gordon supercomputers (OCI-1053575) at the San Diego Supercomputing Center.

■ REFERENCES

(1) Sydorenko, N.; Hsung, R. P.; Vera, E. L. *Org. Lett.* **2006**, *8*, 2611.
(2) Woodward, R. B.; Hoffmann, R. *J. Am. Chem. Soc.* **1965**, *87*, 395.
(3) Kirmse, W.; Rondan, N. G.; Houk, K. N. *J. Am. Chem. Soc.* **1984**, *106*, 7989.
(4) Rondan, N. G.; Houk, K. N. *J. Am. Chem. Soc.* **1985**, *107*, 2099.
(5) Dolbier, W. R.; Koroniak, H.; Houk, K. N.; Sheu, C. *Acc. Chem. Res.* **1996**, *29*, 471.
(6) Honda, K.; Lopez, S. A.; Houk, K. N.; Mikami, K. *J. Org. Chem.* **2015**, DOI: 10.1021/acs.joc.5b01361.
(7) Gilchrist, T. L.; Healy, M. A. M. *Tetrahedron* **1993**, *49*, 2543.
(8) Maynard, D. F.; Okamura, W. H. *J. Org. Chem.* **1995**, *60*, 1763.
(9) Smith, D. A.; Ulmer, C. W., II. *J. Org. Chem.* **1991**, *56*, 4444.

(10) Beccalli, E. M.; Clerici, F.; Gelmi, M. L. *Tetrahedron* **2000**, *56*, 4817−4821.
(11) Palacios, F.; Gil, M. J.; de Marigorta, E. M.; Rodríguez, M. *Tetrahedron* **2000**, *56*, 6319.
(12) Tanaka, K.; Katsumura, S. *Yuki Gosei Kagaku Kyokaishi* **2005**, *63*, 696.
(13) Vincze, Z.; Mucsi, Z.; Scheiber, P.; Nemes, P. *Eur. J. Org. Chem.* **2008**, *2008*, 1092.
(14) Liu, S.; Liebeskind, L. S. *J. Am. Chem. Soc.* **2008**, *130*, 6918.
(15) Nakamura, I.; Zhang, D.; Terada, M. *J. Am. Chem. Soc.* **2010**, *132*, 7884.
(16) Nakamura, I.; Zhang, D.; Terada, M. *J. Am. Chem. Soc.* **2011**, *133*, 6862.
(17) Vincze, Z.; Nemes, P. *Tetrahedron* **2013**, *69*, 6269.
(18) For a review on aza-electrocyclizations, see: Okamura, W. H.; de Lera, A. R. In *Comprehensive Organic Synthesis*; Trost, B. M., Fleming, I., Eds.; Pergamon Press: New York, 1991; Vol. *5*, pp 699−750.
(19) Sklenicka, H. M.; Hsung, R. P.; Wei, L.-L.; McLaughlin, M. J.; Gerasyuto, A. I.; Degen, S. J. *Org. Lett.* **2000**, *2*, 1161.
(20) Tanaka, K.; Mori, H.; Yamamoto, M.; Katsumura, S. *J. Org. Chem.* **2001**, *66*, 3099.
(21) Tanaka, K.; Katsumura, S. *J. Am. Chem. Soc.* **2002**, *124*, 9660.
(22) Buchanan, G. S.; Dai, H.; Hsung, R. P.; Gerasyuto, A. I.; Scheinebeck, C. M. *Org. Lett.* **2011**, *13*, 4402.
(23) Thompson, S.; Coyne, A. G.; Knipe, P. C.; Smith, M. D. *Chem. Soc. Rev.* **2011**, *40*, 4217.
(24) Sklenicka, H. M.; Hsung, R. P.; McLaughlin, M. J.; Wei, L. I.; Gerasyuto, A. I.; Brennessel, W. B. *J. Am. Chem. Soc.* **2002**, *124*, 10435.
(25) Tanaka, K.; Kobayashi, T.; Mori, H.; Katsumura, S. *J. Org. Chem.* **2004**, *69*, 5906.
(26) Liu, X.; Zhang, N.; Yang, J.; Liang, Y.; Zhang, R.; Dong, D. *J. Org. Chem.* **2013**, *78*, 3323.
(27) Tanaka, K.; Yokoi, S.; Morimoto, K.; Iwata, T.; Nakamoto, Y.; Nakayama, K.; Koyama, K.; Fujiwara, T.; Fukase, K. *Bioorg. Med. Chem.* **2012**, *20*, 1865.
(28) Tanaka, K.; Fukase, K.; Katsumura, S. *Chem. Rec.* **2010**, *10*, 119.
(29) Walker, M. J.; Hietbrink, B. N.; Thomas, B. E.; Nakamura, K.; Kallel, E. A.; Houk, K. N. *J. Org. Chem.* **2001**, *66*, 6669.
(30) Houk, K. N.; Moses, S. R.; Wu, Y. D.; Rondan, N. G.; Jager, V.; Schohe, R.; Fronczek, F. R. *J. Am. Chem. Soc.* **1984**, *106*, 3880.
(31) Wiberg, K. B.; Murcko, M. A.; Laidig, K. E.; MacDougall, P. J. *J. Phys. Chem.* **1990**, *94*, 6956.
(32) Goodman, L.; Gu, H. B.; Pophristic, V. *J. Phys. Chem. A* **2005**, *109*, 1223.
(33) Houk, K. N.; Duh, H. Y.; Wu, Y. D.; Moses, S. R. *J. Am. Chem. Soc.* **1986**, *108*, 2754.
(34) Raimondi, L.; Wu, Y. D.; Brown, F. K.; Houk, K. N. *Tetrahedron Lett.* **1992**, *33*, 4409.
(35) Haller, J.; Strassner, T.; Houk, K. N. *J. Am. Chem. Soc.* **1997**, *119*, 8031.
(36) Haller, J.; Niwayama, S.; How-Yunn Duh, A.; Houk, K. N. *J. Org. Chem.* **1997**, *62*, 5728.
(37) Annunziata, R.; Benaglia, M.; Cinquini, M.; Cozzi, F.; Raimondi, L. *Eur. J. Org. Chem.* **1998**, *1998*, 1823.
(38) Lambert, J. B.; Zhao, Y.; Emblidge, R. W.; Salvador, L. A.; Liu, X. Y.; So, J. H.; Chelius, E. C. *Acc. Chem. Res.* **1999**, *32*, 183.
(39) Cieplak, A. S. *J. Am. Chem. Soc.* **1981**, *103*, 4540.
(40) Cieplak, A. S.; Tait, B. D.; Johnson, C. R. *J. Am. Chem. Soc.* **1989**, *111*, 8447.
(41) Wu, Y. D.; Houk, K. N. *J. Am. Chem. Soc.* **1987**, *109*, 908.
(42) Houk, K. N. *Chem. Rev.* **1976**, *76*, 1.
(43) Ma, Z.-X.; Patel, A.; Houk, K. N.; Hsung, R. P. *Org. Lett.* **2015**, *17*, 2138.
(44) Frisch, M. J.; Trucks, G. W.; Schlegel, H. B.; Scuseria, G. E.; Robb, M. A.; Cheeseman, J. R.; Scalmani, G.; Barone, V.; Mennucci, B.; Petersson, G. A.; Nakatsuji, H.; Caricato, M.; Li, X.; Hratchian, H. P.; Izmaylov, A. F.; Bloino, J.; Zheng, G.; Sonnenberg, J. L.; Hada, M.; Ehara, M.; Toyota, K.; Fukuda, R.; Hasegawa, J.; Ishida, M.; Nakajima, T.; Honda, Y.; Kitao, O.; Nakai, H.; Vreven, T.; Montgomery, J. A., Jr.; Peralta, J. E.; Ogliaro, F.; Bearpark, M.; Heyd, J. J.; Brothers, E.; Kudin, K. N.; Staroverov, V. N.; Kobayashi, R.; Normand, J.; Raghavachari, K.; Rendell, A.; Burant, J. C.; Iyengar, S. S.; Tomasi, J.; Cossi, M.; Rega, N.; Millam, J. M.; Klene, M.; Knox, J. E.; Cross, J. B.; Bakken, V.; Adamo, C.; Jaramillo, J.; Gomperts, R.; Stratmann, R. E.; Yazyev, O.; Austin, A. J.; Cammi, R.; Pomelli, C.; Ochterski, J. W.; Martin, R. L.; Morokuma, K.; Zakrzewski, V. G.; Voth, G. A.; Salvador, P.; Dannenberg, J. J.; Dapprich, S.; Daniels, A. D.; Farka, Ö.; Foresman, J. B.; Ortiz, J. V.; Cioslowski, J. *Gaussian 09*, revision D.01.; Gaussian Inc.: Wallingford, CT, 2010.
(45) Zhao, Y.; Truhlar, D. G. *Theor. Chem. Acc.* **2008**, *120*, 215.
(46) Pieniazek, S. N.; Clemente, F. R.; Houk, K. N. *Angew. Chem.* **2008**, *120*, 7860.
(47) Zhao, Y.; Truhlar, D. G. *Acc. Chem. Res.* **2008**, *41*, 157.
(48) Zhao, Y.; Truhlar, D. G. *Phys. Chem. Chem. Phys.* **2008**, *10*, 2813.
(49) Ribeiro, R. F. R.; Marenich, A. V. A.; Cramer, C. J. C.; Truhlar, D. G. D. *J. Phys. Chem. B* **2011**, *115*, 14556.
(50) Weigend, F.; Ahlrichs, R. *Phys. Chem. Chem. Phys.* **2005**, *7*, 3297−3305.
(51) Weigend, F. *Phys. Chem. Chem. Phys.* **2006**, *8*, 1057−1065.
(52) Hanwell, M. D.; Curtis, D. E.; Lonie, D. C.; Vandermeersch, T.; Zurek, E.; Hutchison, G. R. *J. Cheminf.* **2012**, *4*, 17.
(53) *Avogadro: an open-source molecular builder and visualization tool*, version 1.1.1; http://avogadro.openmolecules.net/.
(54) Dennington, R.; Keith, T.; Millam, J. *GaussView*, version 5; Semichem Inc.: Shawnee Mission, KS, 2009.
(55) *CYLview*, 1.0b; Legault, C. Y. Université de Sherbrooke, 2009 (http://www.cylview.org).
(56) Tietze, L. F.; Neumann, T.; Kajino, M.; Pretor, M. *Synthesis* **1995**, *1995*, 1003−1006.

DOI: 10.1021/acs.joc.5b02085
J. Org. Chem. 2015, 80, 11888−11894